

## Determination of the Molecular and Structural Characteristics of Okenia, Mango, and Banana Starches

C. E. MILLAN-TESTA,<sup>†</sup> M. G. MENDEZ-MONTEALVO,<sup>†</sup> M.-A. OTTENHOF,<sup>‡</sup>  
 I. A. FARHAT,<sup>‡</sup> AND L. A. BELLO-PÉREZ\*<sup>\*,†</sup>

Centro de Desarrollo de Productos Bióticos del IPN, Apartado postal 24 C.P.,  
 62731, Yautepec, Morelos, Mexico, and Division of Food Sciences, University of Nottingham,  
 Sutton Bonington Campus, Loughborough LE12 5RD, United Kingdom

Starches were isolated from nonconventional sources (banana, mango, and okenia) and their characteristics were examined using polarized light microscopy, X-ray diffraction pattern, Fourier transform infrared (FTIR) spectroscopy, and differential scanning calorimetry (DSC). Banana starch granules were of an ellipsoidal shape with size between  $\sim 8$  and  $20 \mu\text{m}$ ; okenia had the smallest granule size, between  $\sim 2$  and  $5 \mu\text{m}$ . The three starches showed the Maltese cross, indicative of an intact granule structure. Okenia and mango starches had the A-type X-ray diffraction pattern, common to native cereal starches, whereas banana starch showed a mixture between A- and B-type pattern. Banana starch had the highest temperature ( $77.6 \text{ }^\circ\text{C}$ ) and enthalpy ( $23.4 \text{ J/g}$ ) of gelatinization in excess water conditions; okenia had the lowest temperature ( $71.2 \text{ }^\circ\text{C}$ ) and enthalpy ( $15 \text{ J/g}$ ), which may be related to the X-ray diffraction pattern and its small granule size. Both the okenia and mango starches had a higher molar mass and gyration radius than banana starch, which may be related to the differences determined in their crystalline structures.

**KEYWORDS:** Starch; molar mass; light microscopy; X-ray diffraction; infrared spectroscopy; differential scanning calorimetry

### INTRODUCTION

Starch is one of the most important biopolymers. It is a polymeric mixture of essentially linear (amylose) and branched (amylopectin)  $\alpha$ -glucans. Starch owes much of its functionality and physical organization into a granular structure to these macromolecules (1). It is of great importance to understand the molecular and structural characteristics of starches so as to suggest possible applications of these polymers in diverse systems. Many different techniques can be used to elucidate these characteristics. These include X-ray diffraction (XRD), which measures the long-range order in a sample, that is, the level of crystallinity. Another technique is Fourier transform infrared (FTIR) spectroscopy, which can determine the short-range order in a sample obtaining information on the molecular bond vibrations, such as the prominent C–O and C–C stretching vibrations for carbohydrates, yielding both qualitative and quantitative information, such as that on the amorphous and crystalline regions of the starch granule. A destructive technique, such as differential scanning calorimetry (DSC), has been used to monitor changes occurring upon heating to the bulk of the sample and is not just a surface technique, as is FTIR. In native starches, it is possible to obtain a phase transition

that is due to the gelatinization process, this being a function of the order and chain length distribution of the amylopectin chain (2). Starch is widely used in many applications after solubilization or dispersion in aqueous media under nondegradative conditions. The average molecular weights of these two components influence the functional properties of starch, as demonstrated in gels (3), extrusion products (4), and starch pastes (5). It is therefore important to have a reproducible technique for measuring these macromolecular features. Recent advances in instrumentation have inspired numerous reports on the structure and properties of native, nondegraded starch components, which have been studied by high-performance size-exclusion chromatography (HPSEC) (6–9), HPSEC coupled with multiangle laser light scattering (MALLS) (10–16), or field flow fractionation (FFF) coupled with MALLS (16, 17). A prerequisite step for determining the molecular weight distribution of amylose and amylopectin and their average molar mass by any of these techniques is the complete dissolution of the starch sample in an appropriate solvent without any degradation of the constituent macromolecules. The fulfillment of this requirement is necessary to get information representative of the initial starch sample. In recent years, nonconventional starches have become of increasing importance because of their potential application in the development of new products or improving their traditional uses. In this sense, okenia (18, 19), mango (20), and banana (21) starches have been studied to

\* To whom correspondence should be addressed. Phone: +54 739 42020; fax: +52 739 41896; e-mail: labellop@ipn.mx.

<sup>†</sup> Centro de Desarrollo de Productos Bióticos del IPN.

<sup>‡</sup> University of Nottingham.

determine their chemical, physicochemical, and functional properties. However, no studies concerning the molecular characterization have been reported to date. In recent years, the structure–function relationship of starches has been shown to be of great importance, as knowledge of the molecular structure can suggest applications for the starch in products to improve their functional characteristics.

The present work analyzed the molecular and structural properties of three nonconventional starches using polarized light microscopy, X-ray diffraction, Fourier transform infrared (FTIR) spectroscopy, differential scanning calorimetry (DSC), and SEC-MALLS techniques.

## MATERIALS AND METHODS

**Starch Isolation.** Mature seeds of *O. hypogaea* were harvested at a local experimental farm. The seeds were washed with distilled water to eliminate dust and other impurities and then were cleaned and stored at 4 °C in a sealed container for further use. Okenia starch was isolated using the method suggested by Adkins and Greenwood (22) and adapted by Sánchez-Hernández et al. (18) and Gonzalez-Reyes et al. (19).

Unripened bananas (*Musa paradisiaca*) from the variety “Macho” were purchased in the local market in Cuautla (Mexico) immediately after harvest without any postharvest treatment. The skin color and size are the parameters used for cutting of the fruit. Unripe mangos (*Mangifera indica* L.) from the cv. Tommy Adkins were also purchased in the local market. Both starches were carefully isolated using a modification of the procedure of Kim et al. (23). The fruits were peeled, cut into 5–6-cm cubes (500 g total wt), immediately rinsed in sodium sulfite solution (1.22 g/L), and then macerated mildly at low speed in a Waring blender (500 g fruit: 500 g solution) for 2 min. The homogenate was consecutively sieved and washed through screens (50 and 100 US mesh) until the wash water (distilled) was free from impurities; it was then centrifuged (Hermle Labortechnik, Z300K, Wehingen, Germany) at  $10800 \times g$  for 30 min. The white-starch sediments were dried in a convection oven (Lab-Line Instruments, Inc., Imperial V, Melrose Park, IL) at 40 °C for 48 h, carefully ground with a mortar and pestle to pass through a U.S. no. 100 sieve, and stored at room temperature (25 °C) in a glass container (21, 24).

**Amylose Content.** The total amylose content was determined using the colorimetric method suggested by Hoover and Ratnayake (25).

**Light Microscopy.** A small amount of starch was mixed with distilled water and mounted onto a microscope slide with a coverslip and examined by polarized light microscopy (Leitz, Wetzlar, Germany).

**Wide-Angle X-ray Scattering (WAXS).** A Bruker D5005 wide-angle X-ray diffractometer equipped with a copper source operating at 40 kV and 30 mA producing a  $\text{CuK}\alpha$  radiation with a wavelength of 1.54 Å was used. Data was collected over the  $2\theta$  range 4–38° at 0.1° intervals with a scanning rate of 60 s/deg. The spectra were baseline corrected over the 4–38° range and vector normalized utilizing the OPUS 3.0 software (Bruker, U.K.) before calculating the crystallinity indices using the method of Hermans and Weidinger (26). Triplicate measurements were carried out. To be able to compare the crystallinity values obtained from the various starches, the starch samples were equilibrated to 15% (wet weight basis, w.w.b.) moisture content in an 82% relative humidity environment using a saturated salt solution of KBr (27). The level of starch crystallinity is dependent on the moisture content (28–31).

**Fourier Transform Infrared (FTIR) Spectroscopy.** The mid-infrared spectra were collected using a Bruker IFS48 infrared spectrometer (Bruker, U.K.) equipped with a DTGS detector and a heated single reflectance ATR cell with a diamond crystal (Graseby-specac Ltd., U.K.). A sealed sapphire anvil was used that had a rubber O-ring to minimize moisture loss from the samples during measurements. For each spectrum, 32 scans were acquired at a resolution of  $4 \text{ cm}^{-1}$  and co-added. All sample measurements were recorded at a temperature of 25 °C. The ATR cell, excluding the sample compartment that was sealed, was continuously being purged with dry air to minimize the water vapor contribution to the spectra. Spectra were acquired using

the standard direct mode where the background was recorded with no sample in the ATR cell.

Data analysis was carried out using the OPUS 3.0 software (Bruker, U.K.) To analyze the carbohydrate region of the spectra ( $1200\text{--}800 \text{ cm}^{-1}$ ), baseline correction was applied using a single point at  $1900 \text{ cm}^{-1}$ . The spectra were then deconvoluted (32) in the above-mentioned region, where the assumed line shape was Lorentzian, with a deconvolution factor of 750 and a noise reduction factor of 0.2.

**Differential Scanning Calorimetry (DSC).** The temperature and enthalpy of gelatinization of the starches were studied using a differential scanning calorimeter DSC 7 (Perkin-Elmer, U.K.) calibrated with indium and cyclohexane. The samples were weighed (between 9 and 11 mg sample, dry basis) in stainless steel pans, adding distilled water to create excess water conditions (at least 3 times more than the amount of starch). The pans were hermetically sealed and placed on mixing rollers overnight to allow homogeneous hydration of the sample before carrying out the analysis. An empty pan was used as reference. The samples were heated from 0 to 130 °C at a heating rate of 10 °C/min. The gelatinization or peak temperature ( $T_p$ ) and the transition enthalpy ( $\Delta H$ ) were obtained directly using the accompanying Pyris software. Duplicate measurements were carried out.

**SEC-MALLS Study.** The SEC-MALLS procedure, involving an initial solubilization in dimethyl sulfoxide (DMSO) and then in water using a microwave oven for different times, provides a representative sample without altering the degree of polymerization of the polysaccharides (12).

**Dimethylsulfoxide Treatment.** The sample (1 g) was first dissolved in 95% dimethylsulfoxide (DMSO) (20 mL) with magnetic stirring for 3 days at room temperature. The sample was then precipitated with ethanol (60 mL) and stored overnight at 4 °C. The precipitate was filtered over a glass filter (G4) and washed successively with acetone (10 mL) and diethyl ether (10 mL). The precipitate was air-dried under a hood for a few hours to eliminate the solvents and finally dried in vacuo at 45 °C and 50 kPa for 18–20 h (12).

**Solubilization in Water.** The solubilization procedure was begun by the addition of water (20 mL), which had been filtered through 0.1- $\mu\text{m}$  filter paper (Anotop, Whatmann, Maidstone, U.K.), to a dried dispersed starch sample (10 mg), which had been weighed into the Teflon cup of a model 4782 polycarbonate microwave bomb (total volume 45 mL) (Parr Instrument Co., Moline, IL). The sample was maintained for 15 min under nitrogen flow. The capped Teflon cup was then fitted into the bomb, which had its own pressure cap. This assembly was centered inside a 900 W Panasonic microwave oven. The sample was heated for 40, 50, 60, or 70 s at 900 W. The cooling step was carried out by immersion in an ice bath for 30 min, and the sample was centrifuged at  $31200g$  for 20 min at 15 °C. The supernatant solution was filtered through a 5- $\mu\text{m}$  filter paper (Millipore, Bedford, MA) and dilution series were made at room temperature yielding five or six concentrations. These were injected into the DAWN detector (MALLS, Dawn DSP-F, Wyatt Technology Corporation, Santa Barbara, CA) using the microbatch mode. The carbohydrate concentration of the supernatant solution after filtration was measured by the sulfuric acid-ornicol colorimetric method (12). The weight average molecular weight ( $M_w$ ; g/mol) and z-average gyration radius ( $R_G$ ; nm) were determined with the second-order Berry plot using the ASTRA software for Windows, version 4.90.07 (33). Optical alignment was checked over the angular range described using filtered (0.1- $\mu\text{m}$ ) toluene (11, 12).

## RESULTS AND DISCUSSION

**Light Microscopy.** The radial, ordered arrangement of starch molecules in a granule gives it a quasi-crystalline nature, as is evident from the Maltese crosses seen using polarized light microscopy. The center of the cross is at the hilum. Intact granules exhibit a well-defined birefringence pattern with a dark cross. Birefringence implies only a high degree of molecular orientation within the granule and it does not make reference to any particular crystalline form. Birefringence was observed under polarized light. The three starches showed the charac-

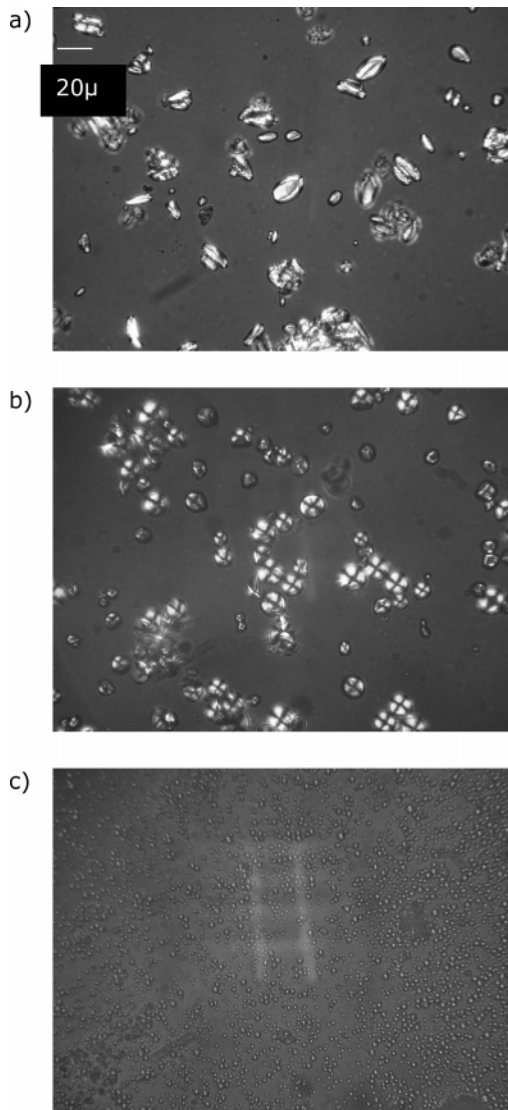


**Figure 1.** Polarized light microscopy of starches from nonconventional sources: (a) banana, (b) mango, (c) okenia.

teristic Maltese crosses, indicating that the isolation method used yielded intact native starch granules.

The banana starch (**Figure 1a**) had granules that were elliptical in shape whereas those obtained from the mango (**Figure 1b**) and okenia (**Figure 1c**) were more spherical. Additionally, the okenia granule size was much smaller than those obtained from banana and mango. The okenia granular size was  $\sim 2\text{--}5\ \mu\text{m}$ , whereas the mango was  $\sim 5\text{--}15\ \mu\text{m}$  and the banana was  $\sim 8\text{--}20\ \mu\text{m}$ .

**Wide-Angle X-ray Scattering (WAXS).** The okenia and mango starches studied gave an A-type X-ray diffraction pattern (**Figure 2**), typically found in native cereal starches. However, the banana starch gave an X-ray pattern that was a mixture between the A- and B-type polymorphs, also referred to as the C-type. In general, legume starches and some tropical tuber starches display the C-type pattern which represents a mixture of A- and B-type crystallinity within the granule (34). Some of the peaks observed with banana starch were similar to those seen with the okenia and mango starches; however, there were also differences believed to indicate the presence of the B-type crystals: the peak observed at a Bragg's angle value of  $2\theta = 5.4^\circ$  (arrow **Figure 2**) was not observed for the other two starches, the peak at  $2\theta = 17^\circ$  was much more prominent than that at  $2\theta = 18^\circ$ , and the peak at  $2\theta = 23^\circ$  was broader. All these differences indicate that the banana starch was a mixture of the A- and B-polymorphs.

The level of crystallinity calculated was very similar for all three starches with values of 36% ( $\pm 2.5\%$ ) obtained for the banana starch and 35% for the mango ( $\pm 1.1\%$ ) and okenia ( $\pm 0.3\%$ ) starches. Lower percentage crystallinities were obtained from different varieties of wheat starches (14), and their values ranged between 13 and 18%. This could be related to the different botanical source of the starch but will also be dependent on the method of calculating the percentage crystallinity. Other authors reported a B-type pattern for banana starch (35, 36) and in another study Jane et al. (37) found that banana starch presented a C-type diffraction pattern, correlating with the results found in this study. The variety of banana starch could play an important role, although the aforementioned authors used *Musa acuminata*, different from the *Musa paradisiaca* species analyzed in this study, yet the results were the same.

**Fourier Transform Infrared (FTIR) Spectroscopy.** The FTIR spectra for the native starches are shown in **Figure 3**. The information obtained from this technique is related to the short-range order in the starch molecule (38). Information on

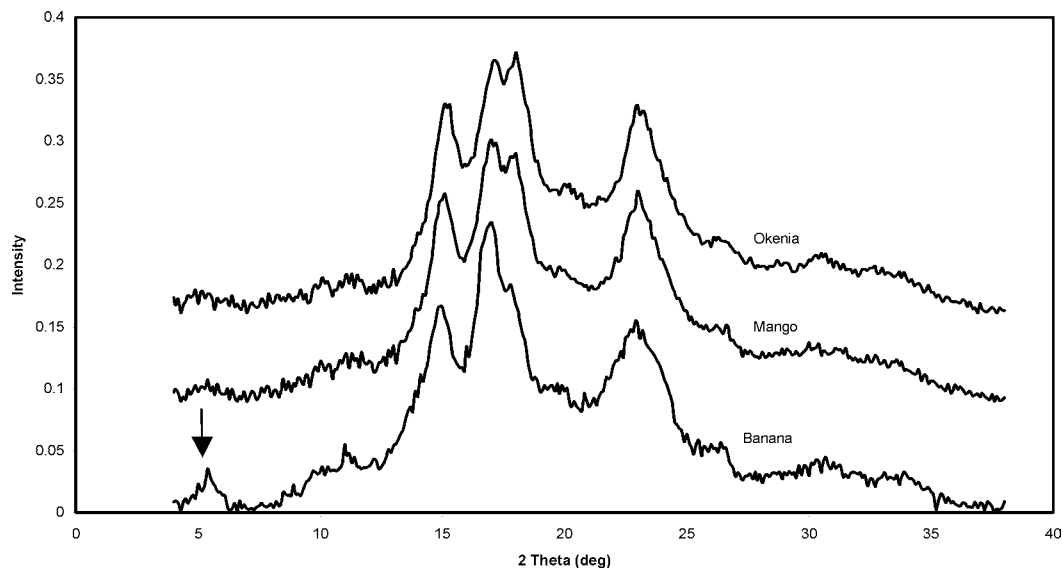


**Figure 2.** X-ray diffraction pattern of starches from nonconventional sources.

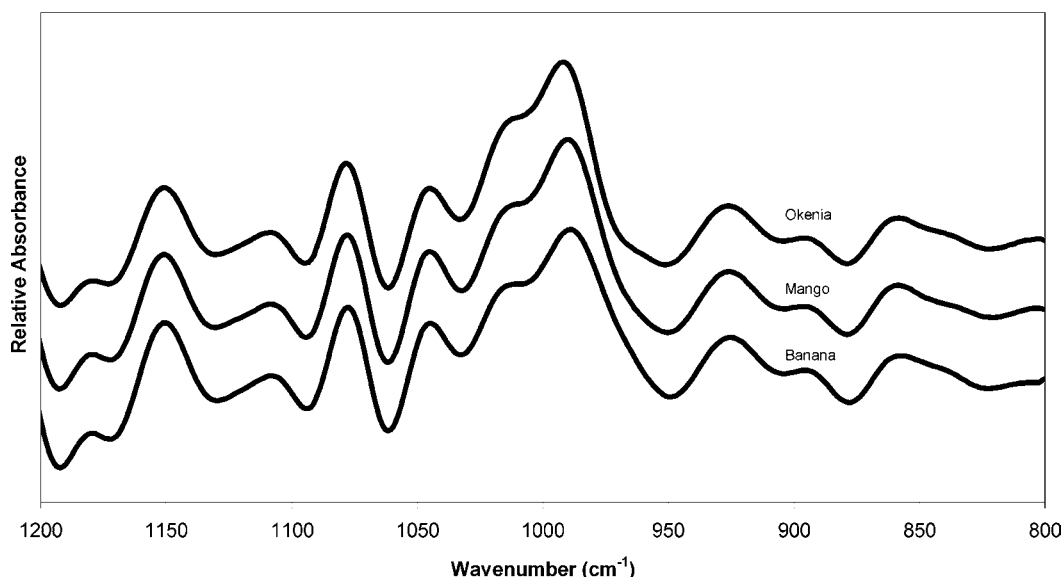


Figure 3. Mid-IR spectra of starches isolated from nonconventional sources

the quantity of ordered and amorphous regions present in the starches is important for knowing the behavior of the polysaccharide when it is being processed, for example, heat treatments, or to predict the characteristics of the starchy products when they are being stored. The ratio between the absorbance obtained at a wavenumber of  $1022\text{ cm}^{-1}$ , related to the amorphous component (39), and that obtained at  $1045\text{ cm}^{-1}$ , related to the ordered component (40), were 1.12, 1.11, and 1.35 for the banana, mango, and okenia starches, respectively. Banana and mango starches contained similar amounts of short-range order, yet they differed from the okenia starch. This could influence some of the physicochemical, functional, and digestibility characteristics of these materials.

With ATR-FTIR, the infrared beam only penetrates the first  $\sim 2\text{ }\mu\text{m}$  of a sample; it is a surface measurement technique. The spectra obtained of native starches with ATR-FTIR differed depending on the botanical source of the starch (38). Sevenou et al. (38) found that the band at  $1022\text{ cm}^{-1}$  was less prominent in B-type starches (potato and amylo maize) than in A-type starches (wheat, maize, and waxy maize) and the band at  $995\text{ cm}^{-1}$  was more prominent. They stated that FTIR was not able to differentiate between the A- and B-type crystal polymorphs, as FTIR was only sensitive to short-range order. They attributed these differences to the fact that the external regions of the B-type starches they analyzed were more ordered than those of the A-type starches. The ratio of the bands  $1022:995\text{ cm}^{-1}$  for the banana, mango, and okenia starches yielded values of 0.59, 0.51, and 0.50, respectively. From these values, the mango and okenia starches were very similar. The banana starch was slightly less ordered in the external region of the granule.

**Differential Scanning Calorimetry (DSC).** DSC was used to study the gelatinization behavior of the banana, mango, and okenia starches (Table 1). Okenia starch had the lowest gelatinization peak temperature and banana the highest one. In the gelatinization enthalpy, banana and mango presented the highest enthalpy values (23.4 and 21.2 J/g, respectively), but without statistical differences ( $\alpha = 0.05$ ). Okenia starch had the lowest enthalpy value of the three starches studied (15.0 J/g). This single transition corresponds to the dissociation of the amylose and amylopectin molecules within the starch granules and leaching out of amylose to the continuous phase (41–43). For banana starch that had the highest gelatinization temperature, this behavior can be in agreement with the different

Table 1. Thermal Analysis (Gelatinization) of Starches Isolated from Nonconventional Sources<sup>a</sup>

sample	$T_p$ (°C)	$\Delta H$ (J/g)
banana	77.6	23.4
mango	73.8	21.2
okenia	71.2	15.0

<sup>a</sup> Data are means;  $n = 2$ .

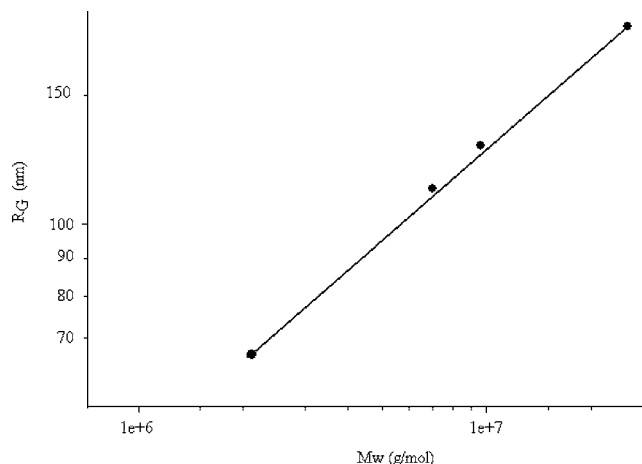
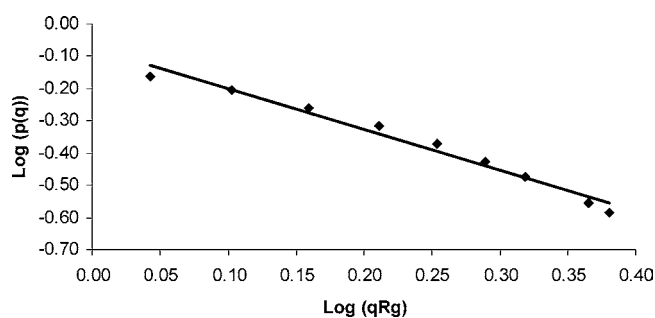
X-ray diffraction pattern (A/B-type) shown, because it was reported that the level of crystallinity and in consequence the diffraction pattern is attributed to the chain length of the amylopectin molecule (44). On the other hand, Yuan et al. (2) reported that amylopectins present in corn starches with longer chains had higher gelatinization temperatures than those amylopectins with shorter chains. This may be the cause of the different pattern observed for the starches analyzed. Additionally, other researchers (45, 46) have found that the A-polymorph was favored by shorter chain lengths, whereas the B-polymorph was favored by longer chain lengths. Native A-type starches tend to have shorter average chain lengths than B-type starches (45–47). As the banana starch was the only starch to show a mixture of the A- and B-type crystal polymorphs (the mango and okenia starches only showed the A-type), this could indicate that it had longer average chain lengths than the other two starches studied. When the DSC trace was obtained for banana starch (data not shown), a shoulder was found at a temperature of  $80\text{ }^\circ\text{C}$ . This event could be due to the existence of two different starch granule populations that are gelatinized at different temperatures. Faisant et al. (36) reported DSC traces for raw green-banana flour. They found a gelatinization temperature of  $69.4\text{ }^\circ\text{C}$  and a gelatinization enthalpy of 17.1 J/g. Both values were lower than those found in this work. Additionally, Bello-Pérez et al. (21) reported gelatinization temperatures of 74.5 and  $75.0\text{ }^\circ\text{C}$  for two banana starches, close to that determined in this study, but the enthalpy values were lower (13.0 and 14.8 J/g). Gonzalez-Reyes et al. (19) reported a gelatinization temperature of  $71.3\text{ }^\circ\text{C}$  and a gelatinization enthalpy of 11.9 J/g for okenia starch. Their gelatinization temperature value was similar to that determined in this work, but the enthalpy value was lower. For mango starch, until today there are no reported results of calorimetric studies.

**Table 2.** Macromolecular Characteristics of Starches Isolated from Nonconventional Sources and Studied by SEC-MALLS

sample	heating time (s)	$M_w$ ( $\times 10^{-6}$ ) (g/mol)	$R_G$ (nm)	$d'_f$	$d_f$
mango	40	13.9	145	1.95	2.81
	50	17.8	147	2.17	
	60	3.9	95	1.27	
	70	1.3	60	0.82	
okenia	40	25.4	186	2.29	2.42
	50	9.6	128	1.87	
	60	7.0	112	1.91	
	70	2.1	67	0.89	
banana	40	6.7	106	1.25	3.74
	50	3.4	92	1.27	
	60	1.9	76	1.32	
	70	0.2	73	1.16	

**SEC-MALLS Study.** The macromolecular characteristics of the starches using different solubilization times are shown in **Table 2**. Generally, as the heating time in the microwave increased, the molar mass ( $M_w$ ) and gyration radius ( $R_G$ ) decreased. This behavior is due to the longer heating times, where degradation of the molecules occurs. Bello-Pérez et al. (12) reported a similar pattern for their starch studied, with  $M_w$  values for normal maize that ranged between  $19 \times 10^7$  g/mol for 35 s of heating to  $2.7 \times 10^7$  g/mol at 90 s of heating and  $R_G$  ranging from 250 nm at 35 s to 100 nm for 90 s. Banana starch had the lowest  $M_w$  and  $R_G$  values of the starches analyzed. The starch that had the lowest  $M_w$  also had the lowest  $R_G$ . The  $M_w$  and  $R_G$  decreased as the amylose content increased as banana had an amylose content of 37%, mango 35%, and okenia 27%. It has been reported that the  $M_w$  of amylopectin decreased as the amylose content increased (13). If the results obtained are compared with those obtained for yam starches (16) solubilized for 40 s, the  $M_w$  and  $R_G$  values were higher, ranging between  $3.41$  and  $0.75 \times 10^8$  g/mol and 396 and 170 nm, respectively, depending on the variety used for starch isolation. The differences found could be due to differences in the starch source and the technique used, as they used an HPSEC-MALLS-RI system. The DMSO treatment for the starches and solubilization time were similar to those used in this study. The  $M_w$  and  $R_G$  values obtained for wheat starches determined with an HPSEC-MALLS-RI system were in the range of  $3.10$ – $5.24 \times 10^8$  g/mol and 301–328 nm, respectively (13), and for amylopectins isolated from maize starches, the  $M_w$  and  $R_G$  values ranged between  $4.9$  and  $8.3 \times 10^8$  g/mol and 312–372, respectively, showing that amylopectin isolated from waxy maize had the highest values of these parameters. Another study using the microbatch mode of the MALLS detector reported  $M_w$  and  $R_G$  values higher for amylopectins isolated from various wheat cultivars than those obtained with chromatography (48). These values were also higher than those found in this work.

**Figure 4** shows the  $M_w$  dependence of the  $R_G$  for okenia starch treated for four different time periods. Similar results were also obtained for banana and mango starches (data not shown). Within the limits of experimental error, the relationship of  $M_w$  to  $R_G$  follows a common straight line on a double logarithmic plot ( $r = 0.94$ ), describing the power law behavior  $R_G = K M_w^{\nu}$ , as already shown by Hanselmann et al. (49), who stated that

**Figure 4.** Molecular weight dependence of the gyration radius ( $R_G$ ) of okenia starch dissolved for different time periods.**Figure 5.** Double logarithmic plot of particle-scattering factor vs the normalized scattering vector of mango starch dissolved for 60 s.

the  $M_w$  dependence of  $R_G$  was according to the following power law:

$$M = K' R_G^{1/\nu} \quad R_G = K'' R_G^{d'_f}$$

The calculated slope values ( $\nu_{RG}$ ) were 0.27, 0.36, and 0.41 and  $d'_f$  values were 3.74, 2.81, and 2.42 for the banana, mango, and okenia starches, respectively. A  $d'_f$  value of 3.0 would define a globular homogeneous structure whereas a  $d'_f$  value of 2.0 would define a planar structure. Bello-Pérez et al. (11, 12) found  $d'_f$  values of 2.77 and 2.70 for corn amylopectin and normal corn, respectively, and a value of 2.56 for amaranth starch. The values determined in this study demonstrated structural differences in the starches from diverse botanical origins.

In **Figure 5**, the particle-scattering factor  $P(q)$ , which describes the angular distribution of the scattered light from mango starch heated for 60 s, is plotted against the dimensionless parameter  $u$  ( $\equiv qR_G$ ), where  $q$  is a scattering vector (50):  $q = (4\pi n/\lambda) \sin(\theta/2)$ . Information about the structure of polymers can be obtained from  $p(q)$ , which describes the angular distribution of the scattered light. The theory of fractals (51) relates this asymptotic slope to a fractal dimension. In this experiment,  $d'_f$  is focusing on the internal structure in contrast to  $d_f$ , which is related to the global structure (49). In both the mango and okenia starches, these slopes showed a dependence on the treatment time (**Table 2**). The values of  $d'_f$  for the samples studied are near to that value characteristic of a particle that has an internal structure of a fully swollen, randomly branched macromolecule in a thermodynamically good solvent ( $d'_f = 2.0$ ) (49). Bello-Pérez et al. (11) reported  $d'_f$  values for amaranth starch dissolved for 35, 50, 70, and 90 s of 2.44, 2.18, 1.50, and 1.03, respectively. A pattern similar to that was found in this study, using static light scattering equipment.

**Conclusions.** The starches studied from banana, mango, and okenia had differently shaped and sized granules but under polarized light showed the Maltese cross, indicating that the isolation procedure yielded intact granules. Banana starch had an X-ray diffraction pattern that was a mixture between the A- and B-type, whereas the mango and okenia starches were of the A-type. Banana starch had the highest temperature and enthalpy of gelatinization, a parameter important in starch applications. The molar mass and gyration radius were higher for mango and okenia starches and the lowest values were determined in banana starch. These molecular parameters decreased when heating time increased because of sample degradation in the microwave. The higher  $d_f$  values for banana starch (3.74) showed structural differences between the starches, as this value would define a globular homogeneous structure, whereas the  $d_f$  values obtained for the mango and okenia starches define a planar structure. The results obtained yielded information about the possible behavior of these starches when being used in certain applications.

#### LITERATURE CITED

- French, A. D. Organization of starch granules, starch. In *Chemistry and technology*; Whistle, R. L., BeMiller, R. L., Paschall, E. F., Eds.; Academic Press: New York, 1984; pp 183–247.
- Yuan, R. C.; Thompson, D. B.; Boyer, C. D. The fine structure of amylopectin in relation to gelatinization and retrogradation behavior of maize starches from three wx-containing genotypes in two inbred lines. *Cereal Chem.* **1993**, *70*, 81–89.
- Clark, A. H.; Gidley, M. J.; Richardson, R. K.; Ross-Murphy, S. B. Rheological studies of aqueous amylose gels: the effect of chain length and concentration on gel modulus. *Macromolecules* **1989**, *22*, 346–351.
- Della-Valle, G.; Colonna, P.; Patria, A.; Vergnes, B. Influence of amylose content on the viscous behavior of low hydrated molten starches. *J. Rheol.* **1996**, *40*, 347–362.
- Doublier, J. L.; Colonna, P.; Mercier, C. Extrusion cooking and drum drying of wheat starch. II: rheological characterization of starch pastes. *Cereal Chem.* **1986**, *63*, 240–246.
- Takeda, C.; Takeda, Y.; Hizukuri, S. Structure of the amylopectin fraction of amylo maize. *Carbohydr. Res.* **1993**, *246*, 273–281.
- Ong, M. H.; Blanshard, M. V. Texture determinants in cooked, parboiled rice I: rice starch amylose and the fine structure of amylopectin. *J. Cereal Sci.* **1995**, *21*, 251–260.
- Striegel, A. M.; Timpa, J. D. Molecular characterization of polysaccharides dissolved in Me<sub>2</sub>NAC-LiCl by gel-permeation chromatography. *Carbohydr. Res.* **1995**, *267*, 271–290.
- Hizukuri, S. Polymodal distribution of the chain lengths of amylopectins, and its significance. *Carbohydr. Res.* **1986**, *147*, 342–347.
- Fishman, M. L.; Rodriguez, L.; Chau, H. K. Molar masses and sizes of starches by high-performance size-exclusion chromatography with on-line multi-angle laser light scattering detection. *J. Agric. Food Chem.* **1996**, *44*, 3182–3188.
- Bello-Pérez, L. A.; Colonna, P.; Roger, P.; Paredes-Lopez, O. Macromolecular features of amaranth starch. *Cereal Chem.* **1998**, *75*(4), 395–402.
- Bello-Pérez, L. A.; Roger, P.; Baud, B.; Colonna, P. Macromolecular features of starches determined by aqueous high-performance size exclusion chromatography. *J. Cereal Sci.* **1998**, *27*, 267–278.
- Yoo, S. H.; Jane, J. Structural and physical characteristics of waxy and other wheat starches. *Carbohydr. Polym.* **2002**, *49*, 297–305.
- Yoo, S. H.; Jane, J. Molecular weights and gyration radii of amylopectins determined by high-performance size-exclusion chromatography equipped with multi-angle laser-light scattering and refractive index detectors. *Carbohydr. Polym.* **2002**, *49*, 307–314.
- Ji, Y.; Wong, K.; Hasjim, J.; Pollak, L. M.; Duvick, S.; Jane, J.; White, P. J. Structure and function of starch from advanced generations of new corn lines. *Carbohydr. Polym.* **2003**, *54*, 305–319.
- Rolland-Sabaté, A.; Amai, N. G.; Dufour, D.; Guilois, S.; Colonna, P. Macromolecular characteristics of ten yam (*Dioscorea spp*) starches. *J. Sci. Food Agric.* **2003**, *83*, 927–936.
- Roger, P.; Baud, B.; Colonna, P. Characterization of starch polysaccharides by flow field-flow fractionation-multi angle laser light scattering-differential refractometer index. *J. Chromatogr., A* **2001**, *9*(17), 179–185.
- Sanchez-Hernández, L.; Solorza-Feria, J.; Méndez-Montealvo, G.; Paredes-López, O.; Bello-Pérez, L. A. Isolation and partial characterization of okenia (*Okenia hipogaea*). *Starch/Staerke* **2002**, *54*, 193–197.
- González-Reyes, E.; Méndez-Montealvo, G.; Solorza-Feria, J.; Toro-Vazquez, J. F.; Bello-Pérez, L. A. Rheological and thermal characterization of *Okenia hypogaea* (Schlech. & Cham.) starch. *Carbohydr. Polym.* **2003**, *52*, 297–310.
- Bello-Pérez, L. A.; Aparicio-Saguilán, A.; Méndez-Montealvo, G.; Solorza-Feria, J.; Flores-Huicochea, E. Isolation and partial characterization of mango (*Mangifera indica L.*) starch: morphological, physicochemical and functional studies. *Plant. Foods Hum. Nutr.* **2004**, accepted for publication.
- Bello-Pérez, L. A.; Agama-Acevedo, E.; Sánchez-Hernández, L.; Paredes-López, O. Isolation and partial characterization of banana. *Starch/Staerke* **1999**, *47*, 854–857.
- Adkins, G. K.; Greenwood, C. T. The Isolation of cereal starches in the laboratory. *Starch/Staerke* **1966**, *7*, 213–218.
- Kim, S.; Wiesenborn, D. P.; Orr, P. H.; Grant, L. A. Screening potato starch for novel properties using differential scanning calorimetry. *J. Food Sci.* **1995**, *60*, 1060–1065.
- Aparicio-Saguilán, A. Aislamiento y caracterización parcial de almidón de mango (*Mangifera indica*). B.S.c Thesis, Instituto Tecnológico de Acapulco, México, 2001.
- Hoover, R.; Ratnayake, W. S. Starch characteristics of black bean, chick pea, lentil navy bean and pinto bean cultivars grown in Canada. *Food Chem.* **2002**, *78*, 489–498.
- Hermans, P. H.; Weidinger, A. Quantitative X-ray investigations on the crystallinity of cellulose fibers: a background analysis. *J. Appl. Phys.* **1948**, *19*, 491–506.
- Nyqvist, H. Saturated salt solutions for maintaining specified relative humidities. *Int. J. Pharm. Techn. Prod. Manufac.* **1983**, *4*, 47–48.
- Buleon, A.; Bizot, H.; Delage, M. M.; Multon, J. L. Evolution of crystallinity and specific gravity of potato starch versus water ad- and desorption. *Starch/Staerke* **1982**, *34*, 361–366.
- Nara, S.; Komiya, T. Studies on the relationship between water-saturated state and crystallinity by the diffraction method for moistened potato starch. *Starch/Staerke* **1983**, *35*, 407–410.
- Chinachoti, P.; Steinberg, M. P. Crystallinity of waxy maize starch as influenced by ambient-temperature absorption and desorption, sucrose content and water activity. *J. Food Sci.* **1986**, *51*, 997.
- Buleon, A.; Le Bail, P.; Colonna, P.; Bizot, H. Phase and polymorphic transitions of starches at low and intermediate water contents. In *The properties of water in foods*; Reid, D. S., Ed.; Blackie Academic & Professional: London, 1998; pp 160–178.
- Kauppinen, J. K.; Moffatt, D. J.; Mantsch, H. H.; Cameron, D. G. Fourier self-deconvolution: a method for resolving intrinsically overlapped bands. *Appl. Spectrosc.* **1981**, *35*(3), 271–276.
- Wyatt, P. J. Light scattering and the absolute characterization of macromolecules. *Rev. Anal. Chim. Acta* **1993**, *272*, 1–40.
- Spencer, K. E.; Jane, J. Chemical and physical properties of ginkgo (*Ginkgo biloba*) starch. *Carbohydr. Polym.* **1999**, *40*, 261–269.
- Lii, C. Y.; Chang, S. M.; Young, Y. L. Investigation of the physical and chemical properties of banana starches. *J. Food Sci.* **1982**, *47*, 1493–1497.

- (36) Faisant, N.; Buléon, A.; Colonna, P.; Molis, C.; Lartigue, S.; Galmiche, J. P.; Champ, M. Digestion of raw banana starch in the small intestine of healthy humans: structural features of resistant starch. *Br. J. Nutr.* **1995**, *73*, 111–123.
- (37) Jane, J. L.; Wong, K. S.; McPherson, A. E. Branch-structure difference in starches of A- and B-type x-ray patterns revealed by their Naegeli dextrans. *Carbohydr. Res.* **1999**, *300*, 219–227.
- (38) Sevenou, O.; Hill, S. E.; Farhat, I. A.; Mitchell, J. R. Organisation of the external region of the starch granule as determined by infrared spectroscopy. *Int. J. Biol. Macromol.* **2002**, *31*, 79–85.
- (39) van Soest, J. J.; Tournois, H.; de Wit, D.; Vliegthart, J. F. Short-range structure in (partially) crystalline potato starch determined with attenuated total reflectance Fourier-transform IR spectroscopy. *Carbohydr. Res.* **1995**, *279*, 201–214.
- (40) Smits, A. L.; Ruhnau, F. C.; Vliegthart, J. F.; Van Soest, J. J. Ageing of starch based systems as observed with FT-IR and solid-state NMR spectroscopy. *Starch/Staerke* **1998**, *50*, 478–483.
- (41) Fujita, S.; Lida, T.; Fujiyama, G. Relationship between gelatinization temperature and enthalpy of starch from graminous crops by DSC. *Starch/Staerke* **1992**, *44*, 456–461.
- (42) Liu, H.; Lelièvre, J.; Ayoung, C. W. A study of starch gelatinization using differential scanning calorimetry, x-ray and birefringence measurements. *Carbohydr. Polym.* **1991**, *210*, 175–182.
- (43) Russel, P. L.; Juliano, B. O. Differential scanning calorimetry of rice starches. *Starch/Staerke* **1983**, *35*, 382–386.
- (44) Hizukuri, S. Relationship between the distribution of the chain length of amylopectin and the crystalline structure of starch granules. *Carbohydr. Res.* **1985**, *141*, 295–306.
- (45) Hizukuri, S.; Kaneko, T.; Takeda, Y. Measurement of chain length of amylopectin and its relevance to the origin of crystalline polymorphism of starch granules. *Biochim. Biophys. Acta* **1983**, *760*, 188–191.
- (46) Gidley, M. J. Factors affecting the crystalline type (A-C) of native starches and model compounds: a rationalisation of observed effects in terms of polymorphic structures. *Carbohydr. Res.* **1987**, *161*, 301–304.
- (47) Ong, M. H.; Jumel, K.; Tokarczuk, P. F.; Blanshard, J. M.; Harding, S. E. Simultaneous determinations of the molecular weight distributions of amyloses and the fine structures of amylopectins of native starches. *Carbohydr. Res.* **1994**, *260*, 99–117.
- (48) You, S.; Fredorowicz, M.; Lim, S. T. Molecular characterization of wheat amylopectins by multiangle laser light scattering analysis. *Cereal Chem.* **1999**, *76*, 116–121.
- (49) Hanselman, R.; Burchard, W.; Ehrat, M.; Widmer, H. M. Structural properties of fractionated starch polymers and their dependence on the dissolution process. *Macromolecules* **1996**, *29*, 3277–3282.
- (50) Brown, W.; Nicolai, T. Dynamic properties of polymer solution. In *Dynamic light scattering the method and some applications*; Brown, W. Ed.; Clarendon Press: Oxford, 1993; pp 272–319.
- (51) Stauffer, D. Scaling theory of percolation clusters. *Phys. Rep.* **1979**, *54*, 1–74.

---

Received for review July 9, 2004. Revised manuscript received October 31, 2004. Accepted November 5, 2004. Financial support from the Coordinación General de Posgrado e Investigación-IPN (CGPI-IPN) is gratefully acknowledged.

JF048862X